J Mater Sci: Mater Med (2009) 20:1831–1838
DOI 10.1007/s10856-009-3759-4

Effect of grooves on adsorption of RGD tripeptide onto rutile TiO_2 (110) surface

Mingjun Chen · Chunya Wu · Daiping Song · Wenman Dong · Kai Li

Received: 12 February 2009 / Accepted: 17 April 2009 / Published online: 6 May 2009

Abstract Molecular dynamics (MD) simulations have been performed to investigate the adsorption mechanism of Arg-Gly-Asp (RGD) tripeptide onto perfect and grooved rutile TiO_2 (110) surfaces, respectively. The simulation results suggest that RGD tripeptide can strongly adsorb onto TiO_2 surface through specified Ti coordination sites. Analysis of adsorption energy, mean-squared displacements and radial distribution functions indicates that the adsorption of RGD onto grooved surface is more stable and rapid than that onto the perfect surface, with the adsorption energy around −331.59 kcal/mol. And among the chosen groove surfaces, adsorption energies, adsorption speeds and adsorption depths of RGD onto the surfaces increase evidently with the extension of groove dimensions. For both perfect and grooved surfaces, once bonded to the surfaces by interactions of carboxyl groups or carbonyl groups with nearby surface Ti atoms, RGD tripeptides show a reasonable propensity to remain there and undergo relatively limited hinge-bending motions.

1 Introduction

Ti-based materials are well known to possess unique characteristics responsible for their successful use as medical implants and prosthesis, such as excellent mechanical properties, lack of toxicity, extremely low corrosion rate and good biocompatibility [1], which derive mainly from the presence of a thin and strongly adherent oxide layer with a thickness of 0.5–10.0 nm [2]. As soon as Ti-based biomaterials are implanted into human body, the essential component of the outmost oxide layer, i.e., TiO_2, comes into contact with various proteins in the tissue fluid and blood directly. So the initial surface properties of Ti-based implants determine the adsorption modes of proteins, thereby affecting the binding states between host cells and implant surfaces.

The adsorption mechanisms of different molecules onto TiO_2 surfaces have been widely investigated using both experimental and theoretical methods. The majority of experimental studies on TiO_2 refer to rutile (110), since it is the most stable crystal face with minimum surface energy and single crystal with this surface orientation is available [3]. Meanwhile, more and more progresses have also been made towards the theoretical calculation of molecular adsorption onto various TiO_2 surfaces. However, due to the limit of computational efficiency, which results in a relatively short period of calculation time, and the formidable complexity behind the atomistic description of large molecular ensembles [4], many researchers only focus on calculations of simple molecules, such as water, amino acids and short peptides, with small clusters modeling the TiO_2 surface. Andreas Kornherr [5] presented a model combining ab initio concepts and molecular dynamics simulations for a treatment of associative multilayer adsorption processes of water molecules onto stoichiometric and reduced rutile TiO_2 (110) surfaces. In the same year, Brandura [6] modeled the H_2O–TiO_2 rutile (110) interface, considering both associative and dissociative mechanisms for half-monolayer and monolayer coverages. Langel et al. [7] and Köppen et al. [3] simulated the adsorption of several amino acids onto TiO_2 surfaces.

M. Chen · C. Wu (✉) · D. Song · W. Dong · K. Li
Center for Precision Engineering, Harbin Institute of Technology, Harbin 150001, China
e-mail: wuchunya1982@163.com

M. Chen
e-mail: chenmj@hit.edu.cn

Carravetta and Monti et al. [8, 9] investigated the interactions of TiO_2 and short peptides (alanine-glutamic acid and alanine-lysine) in water solution.

Amino acid sequence Arg-Gly-Asp (RGD) which is expressed in many extracellular matrix proteins, including fibronectin, vitronectin, fibrinogen, von Willebrand factor, Nestin and Collagen, serves as a primary cell attachment cue and modulates the cell adhesion by attaching to integrins of cell surface receptors, i.e., $\alpha_5\beta_1$, $\alpha_x\beta_1$ and $\alpha_3\beta_1$ [10–12]. And the responsibility of RGD sequence for cell attachment has already been extensively documented in the international literatures since Pierschbacher and Ruoslahti laid the foundation in the mid-1980s [13, 14]. It is thus interesting to study the interaction mechanisms that take place in the adsorption process of RGD tripeptides onto TiO_2 surfaces. And Zhang et al. [15] has already attempted to analyze the adsorption of RGD on different titanium oxide surfaces with MD simulation. But the substrate surfaces were typically restricted to perfect ones without any defect. However, the present work here introduces reduced substrate surface by groove in the surface layer in order to investigate and distinguish the adsorption behaviors of RGD in the peptide-TiO_2 interface regions for rutile (110) perfect and grooved models, by means of Larger-scale Atomic/Molecular Massively Parallel Simulator. Furthermore, a detailed analysis of how the surface grooves with various dimensions affecting the adsorption state of RGD is also performed. Adsorption energy, mean-squared displacements (MSDs), and radial distribution functions (RDFs) are adopted to well understand the interaction mechanisms between RGD and rutile TiO_2 (110) surfaces.

2 Methods

The rutile TiO_2 (110) surface contains 5- and 6-fold Ti atoms (Ti_5 and Ti_6, respectively) and two types of oxygen atoms [in-plane three-fold oxygen atoms (O_s) and double coordinated bridging oxygen atoms (O_b)]. The outermost O_b atoms protrude above the surface and are bound to two Ti_6 atoms in the surface plane, while the Ti_5 atoms are coordinated to O_s atoms on the surface. The rutile TiO_2 (110) surface, placed in the x–y plane, was created by periodic replication in the x and y directions of an elementary cell with a dimension of $\sqrt{2}a \times c$,, which corresponds to 6.50 and 2.96 Å along [$\bar{1}$10] and [001] directions, respectively [16, 17], leading to a MD simulation box whose xy-size was 53.26 × 64.97 $Å^2$.

RGD tripeptide deriving from an Arg-Gly-Asp part of fibronectin is shown in Fig. 1. Arg, Gly and Asp residues are electropositive, electroneutral and electronegative, respectively.

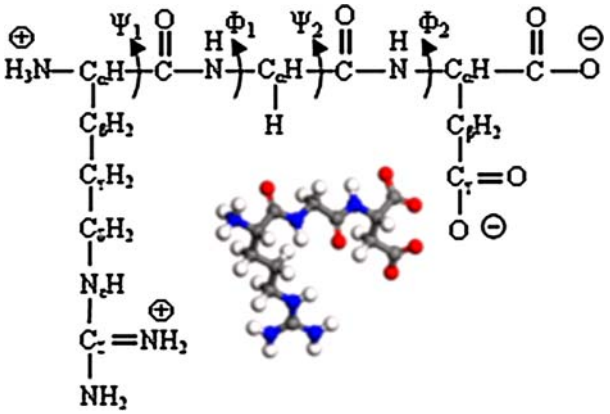

Fig. 1 Structure representation of Arg-Gly-Asp (RGD)

Table 1 lists parameters of simulation models used in our computational investigation. To make a comparison between adsorption processes of RGD tripeptides onto perfect and grooved TiO_2 surfaces in vacuo, model I chosen here is made of rutile TiO_2 (110) perfect surface, comprising 16 layers formed by 5760 Ti, 11520 O atoms, and a fragment of RGD sequence, while the rectangular groove with a dimension of 23.67 × 32.48 × 3.25 $Å^3$ in model II was created by removing 240 atoms from the surface layer of model I, as shown in Fig. 2. The RGD tripeptides were initially placed a bit far from the surface, with the lower-most points at a distance of 25.00 Å from the top layer of TiO_2 for both models, in order to test whether RGD will rotate significantly in the process of deposition.

The two simulation models were carried out at $T = 310.15$ K in canonical ensemble (NVT) using the Nose-Hoover thermostat [18] with a time step of 0.50 fs. Periodic boundary conditions were applied in the x and y directions, with a periodic vacuum gap of 3-fold slab model thickness along z direction. TiO_2 was calculated by using Buckingham potential [19], and AMBER force field [20] was employed to adequately describe peptide structures. Some interactions between TiO_2 and peptide were

Table 1 Simulation parameters for perfect and grooved models

Parameters	Perfect surface	Grooved surface
O atoms	11520	11360
Ti atoms	5760	5680
RGD	1	
Boundary condition	X-, Y-periodic boundary condition; Z-fixed boundary condition	
Simulation temperature	310.15 K	
Time step	0.50 fs	

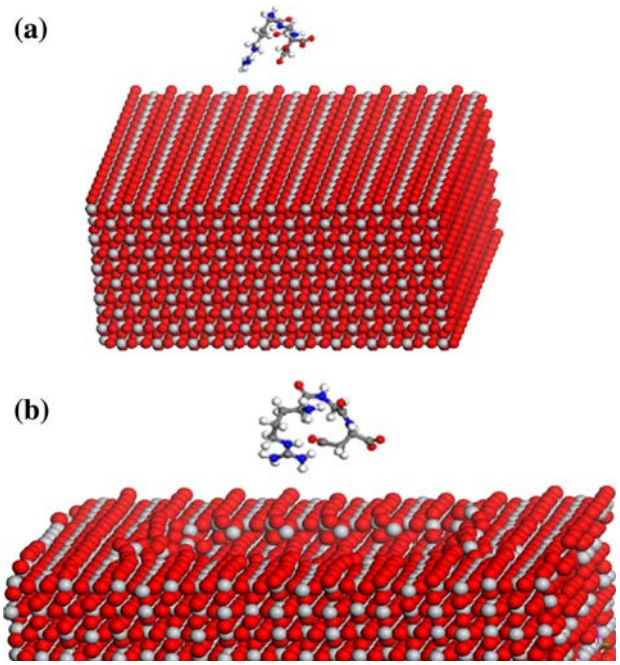

Fig. 2 TiO_2-RGD model. **a** Perfect surface, **b** grooved surface. TiO_2 and RGD are shown by CPK mode and ball-and-stick mode, respectively

described by using a Buckingham potential, while for others a Lennard-Jones potential was used. Simultaneously, SHAKE algorithm [21] was adopted to constrain all bond lengths and bond angles connected to H atoms. The velocity Verlet algorithm was used to calculate the atomic motions and the long-rang electrostatic interactions were handled using particle-particle particle-mesh (PPPM) solver [22]. The two bottom TiO_2 layers were frozen during the whole simulation process. The assemblies made of RGD and TiO_2 were initially energy minimized to remove bad steric contacts at the box boundaries by using Polak-Ribiere version of conjugate gradient algorithm. Then, the systems were allowed to relax at constant temperature and volume over 50 ps with position restraints on the carboxyl oxygen atoms (O_{coo-}) of RGD to prepare the systems in a form such that unphysical forces did not cause improbable displacements. Finally, the resulting conformation of each system was equilibrated for 200 ps without any constraint. During the simulation process, atom coordinates, atom velocities, forces on atoms and energies were all monitored. Every 1 ps a snapshot of the entire system was taken, enabling us to obtain a detailed analysis of the evolution of RGD adsorption onto TiO_2 surfaces as a function of time.

3 Results and discussions

3.1 Comparison of RGD tripeptides adsorption onto perfect and grooved surfaces

According to experimental observations, amino acids easily bind to TiO_2 surface through their carboxyl group [1, 23, 24]. And from theoretical investigations, Langel et al. [7] pointed that O atoms of the carboxyl group formed bonds with surface Ti atoms of the dehydroxylated surfaces. While Monti [9] emphasized that apart from the well-investigated adsorption by deprotonated carboxyl group, carbonyl oxygen atoms as well as nitrogen atoms were all possible coordination sites.

In our simulation, we discover that RGD tripeptide has not rotated significantly during deposition process in either of the two models, and it is in direct contact with perfect surface through the carbonyl oxygen atom (O_{co}) of GLY and two carboxyl oxygen atoms (O_{coo-}) of Asp backbone coordinated to Ti atoms. The distance between surface Ti_5 atom and O_{co} atom is 2.10 ± 0.07 Å, the former digit is the mean of instantaneous values saved within the last 50 ps equilibration stage, and the latter value is the corresponding root-mean-square error (σ), which was obtained by

$$\sigma = \sqrt{\frac{\sum_{i=1}^{n} (x_i - \bar{x})^2}{n-1}} \quad (1)$$

where n is the number of conformations sampled, x_i and $\bar{x}$are instantaneous and mean values of the distances, respectively. And coordination to Ti atoms of two O_{coo-} atoms in a tridentate way has also been found, namely, one of the Asp backbone O_{coo-} atoms is bonded to a Ti_5 atom with Ti–O_{coo-} distance of 1.98 ± 0.06 Å, while the other O_{coo-} atom interacts with two adjacent Ti_6 atoms, with Ti–O_{coo-} distances of 2.13 ± 0.08 Å and 2.17 ± 0.09 Å, respectively. Hence the O_b atom binding with the above two Ti_6 atoms is pushed aside, as shown in Fig. 3a.

For the grooved surface, O_{coo-} atoms in both Asp backbone and side chain are all Ti coordination points. Two O_{coo-} backbone atoms interact with two-three-fold Ti atoms (Ti_3) located at the edge of the groove, with bond lengths of 2.00 ± 0.04 Å and 2.01 ± 0.05 Å, respectively. And the two side chain O_{coo-} atoms form adsorption sites with two adjacent Ti_5 atoms at the bottom of the groove. As Fig. 3b shown, the distances between above Ti_5 atoms and O_{coo-} atoms are 1.97 ± 0.04 and 2.07 ± 0.05 Å, respectively. And it is clear that RGD aligns itself almost parallel to the groove.

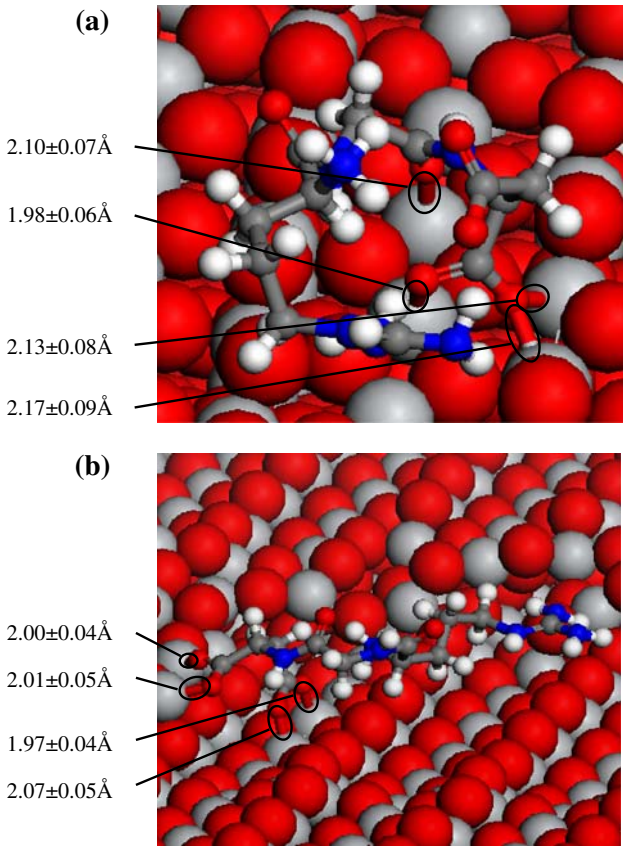

Fig. 3 Adsorption conformations of RGD onto rutile TiO_2 (110) surface. **a** Perfect surface, **b** grooved surface. TiO_2 and RGD are shown by CPK mode and ball-and-stick mode, respectively

3.1.1 Analysis of adsorption energy

As a direct description of surface adsorption capacity, adsorption energy, defined as the energy of the complex minus the energies of the isolated partners is calculated according to Eq. 2, which is exactly opposite to the definition adopted in literature [15]. The above energies were all obtained as average values in MD runs of the corresponding assemblies after equilibration, with each error percentage $\left(\sigma/\bar{x} \times 100\%\right)$ not more than 0.001%. And greater adsorption energy represents more stable adsorption phase.

$$E_{adsorption} = E_{TiO_2+RGD} - (E_{TiO_2} + E_{RGD}) \quad (2)$$

where E_{TiO_2+RGD} is the total energy of RGD–TiO_2 complex, E_{TiO_2} and E_{RGD} are energies of the isolated TiO_2 system and RGD system, respectively.

For perfect surface, where

$$E_{TiO_2} + E_{RGD} = -5274362.42\,\text{kcal/mol}, \quad (3)$$

$$E_{TiO_2+RGD} = -5274497.92\,\text{kcal/mol}, \quad (4)$$

Hence,

$$E_{adsorption} = -5274497.92 - (-5274362.42) = -135.50\,\text{kcal/mol} \quad (5)$$

While for surface with a groove of $23.67 \times 32.48 \times 3.25$ Å^3, where

$$E_{TiO_2} + E_{RGD} = -5208762.16\,\text{kcal/mol}, \quad (6)$$

$$E_{TiO_2+RGD} = -5209093.75\,\text{kcal/mol}, \quad (7)$$

Hence,

$$E_{adsorption} = -5209093.75 - (-5208762.16) = -331.59\,\text{kcal/mol} \quad (8)$$

The adsorption energies of RGD onto perfect and grooved surfaces are −135.50 and −331.59 kcal/mol, respectively. Therefore, the adsorption of RGD onto the grooved surface is more stable than that onto the perfect surface.

3.1.2 Analysis of mean-squared displacements

Mean-squared displacement (MSD) reflecting time-varied displacements of atoms, can readily be evaluated by Eq. 9.

$$MSD(t) = \frac{1}{N}\sum_{j=1}^{N}\left[r_j(t) - r_j(0)\right]^2 \quad (9)$$

where N is the total number of chosen atoms, $r_j(0)$ and $r_j(t)$ are positions of atom j at initial time and t time, respectively.

In this paper, the final conformation of relaxation at constant temperature and volume with position restraints on O_{coo-} of RGD was chosen as the initial state (i.e., $t = 0$) of MSD analysis. And three components of MSD for RGD tripeptides adsorption onto perfect and grooved surfaces, respectively, in the remaining equilibration stage (200 ps) without any constraints are shown in Fig. 4. The x and y directions here are in accordance with the definition of the TiO_2 plane (see Sect. 2), i.e., parallel to the surface, while z direction is perpendicular to the surface. Hence the x, y components represent displacements relative to $t = 0$ of RGD in x–y plane, and the z component corresponds to RGD approaching the surface. As the criteria to evaluate adsorption states, the following definition of equilibration is used: the state of assembly is regarded as equilibration, if the error percentage of energy is not more than 0.001%, and the error percentage of the aggregative MSD (the sum of three components in x, y and z directions) does not exceed 2%. For perfect surface, RGD reaches TiO_2 at ~80 ps, and then adsorbs to the surface without desorption until the final stage of adsorption equilibration. In contrast with perfect surface, RGD approaches the grooved surface more quickly, and reaches the surface at just ~20 ps, then the adsorbed conformation of RGD with attachment to the surface maintains until the end of the simulation. The rutile

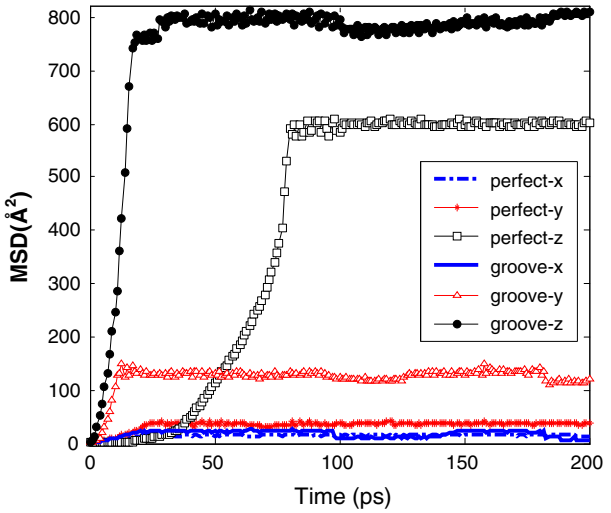

Fig. 4 MSDs for RGD adsorption onto rutile TiO_2 (110) perfect and grooved surfaces

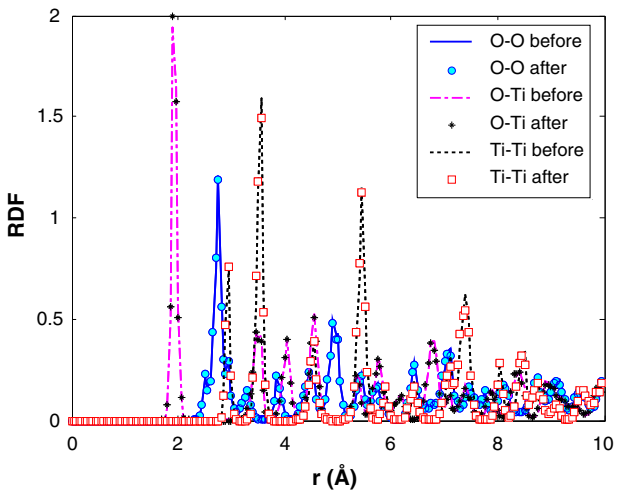

Fig. 5 RDFs of O–O, O–Ti and Ti–Ti. The corresponding values before and after RGD adsorption onto rutile TiO_2 (110) perfect surface are shown by line mode and marker mode, respectively

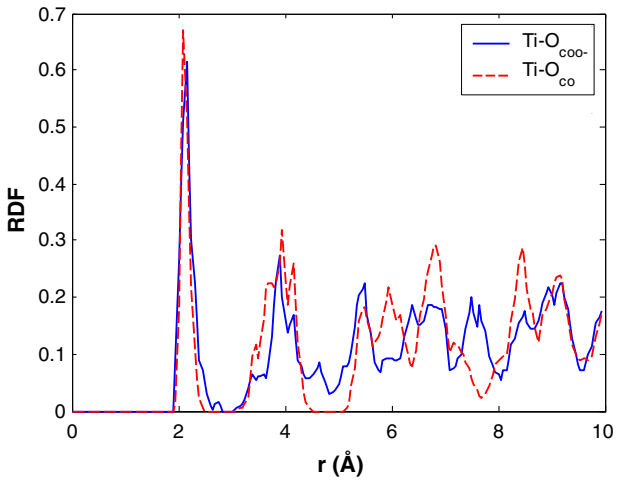

Fig. 6 RDFs of Ti–O_{co} and Ti–O_{coo-} for RGD adsorption onto rutile TiO_2 (110) perfect surface

TiO_2 (110) perfect surface contains only Ti_5 and Ti_6, by contrast, groove edges provide many lower-fold Ti atoms (Ti_3 and Ti_4), which possess higher reactivity and greater attraction to RGD. Therefore, RGD tripeptide does not deposit vertically, but moves towards the groove edge when falling down, and a much larger displacement in y direction may be due to the dimension of the groove, a longer y-length (32.48 Å) compared to x-length (23.67 Å), providing more motion space in y direction for RGD.

3.1.3 Analysis of radial distribution functions

Considering a spherical shell of thickness δr at a distance $r$from a chosen atom, we can obtain the volume of the shell by

$$V = \frac{4}{3}\pi(r+\delta r)^3 - \frac{4}{3}\pi r^3 \approx 4\pi r^2 \delta r \tag{10}$$

Hence, the radial distribution function (RDF), which gives the probability of finding a particle in the distance r from another particle, is given by

$$g(r) = \frac{n(r)}{\rho_0 V} \approx \frac{n(r)}{4\pi\rho_0 r^2 \delta r} \tag{11}$$

where $n(r)$ is the number of atoms appearing in the shell, ρ_0 is the atomic intensity.

RDFs of surface oxygen (O)–O, O–Ti, Ti–Ti, Ti–O_{co} and Ti–O_{coo-}, which were obtained after equilibration, are shown in Figs. 5, 6, 7, and 8. The values are all properly normalized through the appropriate density, and the RDFs of O–O, O–Ti and Ti–Ti before and after RGD adsorbing onto the surface are visualized in the same figure by being symbolized as different markers and line styles, respectively. For perfect surface, a high degree of resemblance between the distribution trends of O–O, O–Ti and Ti–Ti RDFs before and after RGD adsorption can be discovered easily. And the first sharp peaks of O–O, O–Ti and Ti–Ti center at about 2.75, 1.95, and 2.95 Å, respectively, for both states. Thus it is clear that adsorption of RGD does not have a great influence on the crystal structure of TiO_2. The Ti–O_{co} RDFs exhibits a first sharp peak at about 2.05 Å, indicating that O_{co} atoms of GLY is engaged in a direct interaction with the surface Ti atom, as confirmed by Fig. 3. At the same time, the first peak of Ti–O_{coo-} RDF appears at about 2.15 Å, which is a little smaller than the value reported by Zhang et al. (~2.50 Å) [15]. And their stated point that the main contribution of RGD–TiO_2 interaction came from the strong interaction between surface Ti atoms and O_{coo-} atoms of Asp backbone or side chain is slightly different from the results gained by us that

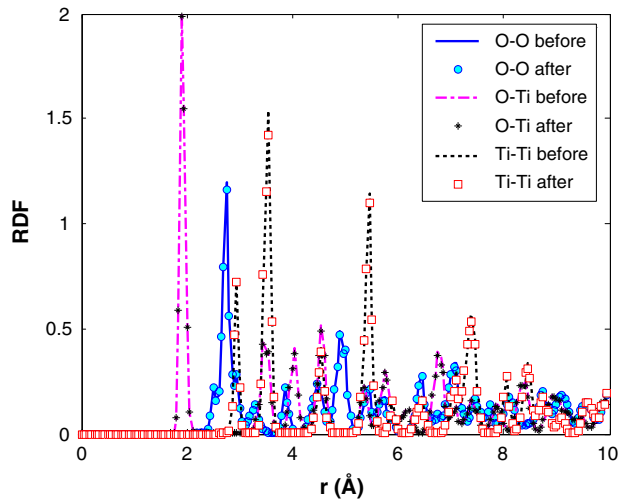

Fig. 7 RDFs of O–O, O–Ti and Ti–Ti. The corresponding values before and after RGD adsorption onto rutile TiO_2 (110) grooved surface are shown by line mode and marker mode, respectively

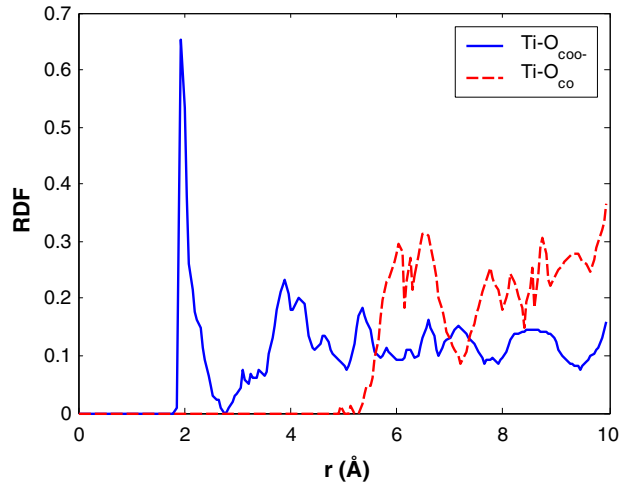

Fig. 8 RDFs of Ti–O_{co} and Ti–O_{coo-} for RGD adsorption onto rutile TiO_2 (110) grooved surface

RGD is in direct contact with perfect rutile surface through O_{co} atom of GLY and two O_{coo-} atoms of Asp backbone coordinated to nearby Ti atoms, which maybe arise from the diversity in initial orientations of RGDs with respect to the surfaces.

Similarly, the O–O, O–Ti and Ti–Ti RDFs are also basically identical before and after RGD adsorbing onto the grooved surface, with first sharp peaks centering at 2.75, 1.95 and 2.95 Å, respectively, showing that no significant change of TiO_2 crystal structure is present to our eyes after RGD adsorbing onto the grooved surface. Ti–O_{coo-} RDF in Fig. 8 has a first sharp neighbor peak centering at 1.95 Å, implying that O_{coo-} atoms of RGD involve in direct bonding interactions with nearby Ti atoms, locating at the edge and bottom surface of the groove. But the distances from O_{co} atoms to Ti atoms are far away from the bond distances suggested by Monti [9]. So no direct coordination of O_{co} to surface atoms exists in the grooved model.

3.2 Impact analysis of groove dimensions on RGD adsorption

The shape and dimension of grooves belonging to implant surfaces have a great influence on cell adsorption. Ponsonnet [25] discovered that the orientation of the cells was related to the surface grooves, the deeper the grooves, the clearer the orientation. And a previous study [26] also showed that the groove depth was more significant to determine cell alignment than width. So we established rutile TiO_2 (110) surface models with rectangular grooves of various dimensions to analyze the impact of groove dimensions on RGD adsorption. Here we just take six models as examples for further analysis. And because space lacks for all complete displays of RGD adsorption onto each surface, Fig. 9 just gives the final states of RGD tripeptides adsorption onto three surfaces with different grooves, whose dimensions are $5.92 \times 32.48 \times 9.75$, $11.84 \times 32.48 \times 6.50$ and $20.71 \times 32.48 \times 12.99$ $Å^3$, respectively. For example, the first two values in $5.92 \times 32.48 \times 9.75$ are lengths of side in x and y directions respectively, while the third value is the depth of groove. As stated in previous section, RGD tripeptide has not rotated significantly during deposition process in both model I and II, where the lower-most points of RGD were facing the surface at a distance of 25.00 Å from the first TiO_2 layer, therefore the RGDs in this section were all placed at a distance of about 5.00 Å from the top layer of TiO_2 surfaces to reduce deposition time, with the same simulation conditions as previous two models.

During the adsorption process, RGD tripeptide moves towards edges and side faces of grooves when depositing. The presence of low-fold Ti atoms improves the adsorption performance of RGD. From Fig. 9, it is obviously that O_{coo-} atoms of RGD always form adsorption sites with Ti atoms, whereas other parts without adsorption undergo relatively limited hinge-bending motions. If the grooves are shallow, O_{coo-} atoms will be coordinated to Ti_3 atoms at the edges of grooves. On the contrary, if the grooves are wide and deep, O_{coo-} atoms will be directly bonded to lower-fold Ti sites at the bottom or side faces. Moreover, lengths of side in x and y directions should be greater than conformational distance between two O_{coo-} atoms of RGD at equilibration time, so as to provide enough conformation space for RGD.

Table 2 gives the simulation information of RGD adsorption onto surfaces with grooves of various dimensions. The deposition time listed is the time span from the initial relaxation without any constraint after the restrained MD of O_{coo-} atoms, to the time point at which RGD

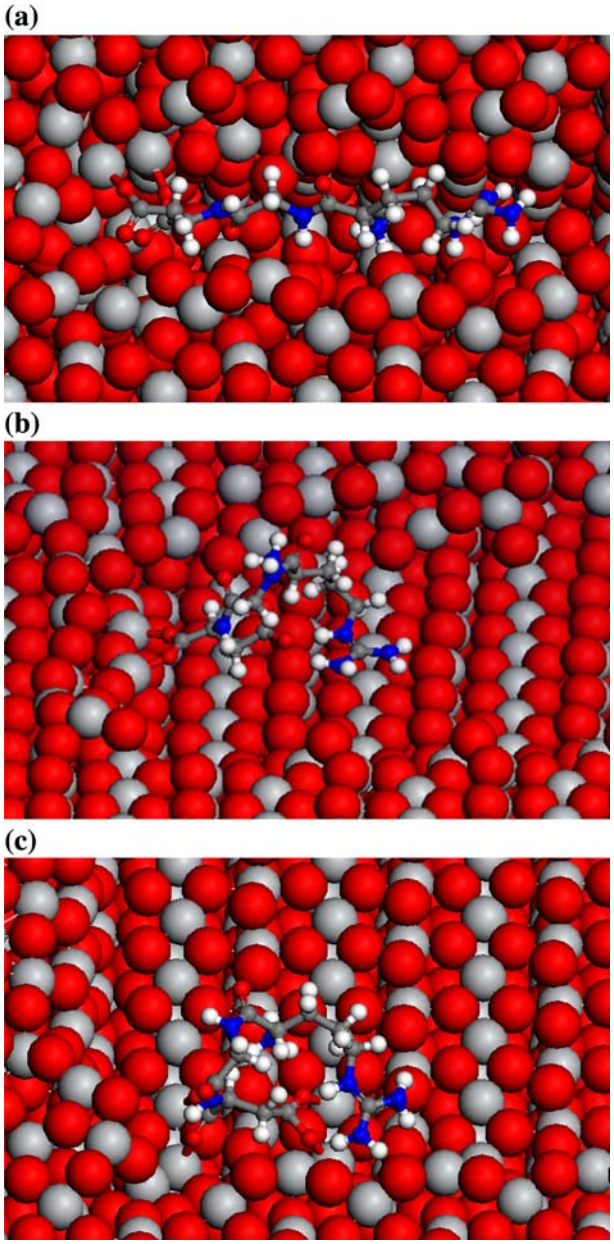

Fig. 9 RGD adsorption onto rutile TiO_2 (110) surfaces with grooves of various dimensions. **a** groove 5.92 × 32.48 × 9.75 Å^3, **b** groove 11.84 × 32.48 × 6.50 Å^3, **c** groove 20.71 × 32.48 × 12.99 Å^3. TiO_2 and RGD are shown by CPK mode and ball-and-stick mode, respectively

exactly comes into contact with the surface. And the MSD provided in the table is the mean of the chosen aggregate values of x, y and z components during the final RGD adsorption equilibration stage. It should be noted that along with the extension of grooves, adsorption energies, adsorption speeds and adsorption depths of RGDs onto the surfaces all increase evidently, possibly due to the following reasons: (i) The presence of groove extends surface area of the material, raises the number of surface atoms,

Table 2 Simulation information of RGD adsorption onto surfaces with various grooves

Grooves	Adsorption energy (kcal/mol)	Deposition time[g] (fs)	MSD[h] (Å^2)
I[a]	−377.21	10700	80.17
II[b]	−410.86	12000	128.43
III[c]	−394.73	12100	346.39
IV[d]	−413.05	13000	406.33
V[e]	−570.41	14100	617.22
VI[f]	−1179.22	14900	888.47

[a] Groove 5.92 × 32.48 × 6.50 Å^3

[b] Groove 5.92 × 32.48 × 9.75 Å^3

[c] Groove 11.84 × 32.48 × 6.50 Å^3

[d] Groove 20.71 × 32.48 × 6.50 Å^3

[e] Groove 20.71 × 32.48 × 12.99 Å^3

[f] Groove 20.71 × 32.48 × 25.99 Å^3

[g] Time span from the initial relaxation without constraint to the time point when RGD exactly comes into contact with the surface

[h] The mean of MSD aggregate values during the final RGD adsorption equilibration stage

and simultaneously increases surface energy rapidly. Hence the surface atoms show high reactivity as a result of the increment of surface atomic number, insufficiency of atomic coordination, and adequacy of surface energy, tending to stabilize by combining with other atoms. (ii) RGD tripeptide will stretch more sufficiently in a larger and deeper groove, so that more energy can be utilized for adsorption.

4 Conclusions

The behavior analysis of RGD tripeptides onto rutile TiO_2 (110) surface reveals significant differences between RGD adsorption onto perfect and grooved surfaces. Carboxyl oxygen atoms of Asp backbone as well as carbonyl oxygen atom of GLY are possible Ti coordination points for perfect surface, while RGD tripeptide attaches to the grooved surface through carboxyl oxygen atoms in both Asp backbone and side chain. Grooved surface is shown to provide higher reactivity adsorption sites, i.e., lower-fold Ti atoms, thereby forming a more stable adsorption state than that onto the perfect surface, with the adsorption energy around −331.59 kcal/mol.

Groove dimension affects the adsorption behavior of RGD tripeptides onto rutile TiO_2 (110) surfaces. Among the finite groove surfaces chosen here, adsorption energies, adsorption speeds and adsorption depths of RGD onto the surfaces increase evidently with the extension of groove dimensions.

For both perfect and grooved surfaces, once bonded to them, RGD has a reasonable propensity to remain there,

with the carboxyl groups or carbonyl groups providing anchors to the surface, while other parts without adsorption undergoing relatively limited hinge-bending motions.

The present paper can be considered as an attempt to obtain behavior information of RGD tripeptide interacting with perfect and grooved TiO_2 surfaces in vacuo. Investigations of RGD tripeptide adsorption onto TiO_2 surfaces in aqueous solution during an extended time span have already been undertaken in our team by the same computational approach.

Acknowledgments This work was supported by the New Century Elitist Supporting Program Foundation by the Ministry of Education of China (No. NCET-06-0332) and the Multidiscipline Scientific Research Foundation of Harbin Institute of Technology (No. HIT. MD 2003. 10).

References

1. Diebold U. The surface science of titanium dioxide. Surf Sci Rep. 2003. doi: 10.1016/S0167-5729(02)00100-0.
2. Jones FH. Teeth and bones: applications of surface science to dental materials and related biomaterials. Surf Sci Rep. 2001. doi: 10.1016/S0167-5729(00)00011-X.
3. Köppen S, Bronkalla O, Langel W. Adsorption configurations and energies of amino acids on anatase and rutile surfaces. J Phys Chem C. 2008. doi: 10.1021/jp803354z.
4. Monti S. Molecular dynamics simulations of collagen-like peptide adsorption on titanium-based material surface. J Phys Chem C. 2007. doi: 10.1021/jp070266t.
5. Kornherr A. Multilayer adsorption of water at a rutile TiO_2 (110) surface: towards a realistic modeling by molecular dynamics. J Chem Phys. 2004. doi: 10.1063/1.1772752.
6. Bandura AV, Sykes DG, Shapovalov V, Troung TN, Kubicki JD, Evarestov RA. Adsorption of water on the TiO_2 (rutile) (110) surface: a comparison of periodic and embedded cluster calculations. J Phys Chem B. 2004. doi: 10.1021/jp037141i.
7. Langel W, Menken L. Simulation of the interface between titanium oxide and amino acids in solution by first principles MD. Surf Sci. 2003. doi: 10.1016/S0039-6028(03)00723-4.
8. Carravetta V, Monti S. Peptide-TiO_2 surface interaction in solution by ab initio and molecular dynamics simulation. J Phys Chem B. 2006. doi: 10.1021/jp056760j.
9. Monti S, Carravetta V, Battocchio C, Iucci G. Peptide/TiO_2 surface interaction: a theoretical and experimental study on the structure of adsorbed ALA-GLU and ALA-LYS. Langmuir. 2008. doi: 10.1021/la702956t.
10. Schaffner P, Dard MM. Structure and function of RGD peptides involved in bone biology. Cell Mol Life Sci. 2003. doi:10.1007/S000180300008.
11. Yao KD, Yin YJ. Biomaterials related to tissue engineering. Beijing: Chemical Industry Press; 2003.
12. Ferris DM, Moodie GD, Dimond PM, Gioranni CWD, Ehrlich MG, Valentini RF. RGD-coated titanium implants stimulate increased bone formation in vivo. Biomaterials. 1999. doi: 10.1016/S0142-9612(99)00161-1.
13. Pierschbacher MD, Ruoslahti E. Cell attachment activity of fibronectin can be duplicated by small synthetic fragments of the molecule. Nature. 1984. doi: 10.1038/309030a0.
14. Ruoslahti E, Pierschbacher MD. New perspectives in cell adhesion: RGD and integrins. Science. 1987. doi:10.1126/science.2821619.
15. Zhang HP, Lu X. Molecular dynamics simulation of RGD peptide adsorption on titanium oxide surfaces. J Mater Sci: Mater Med. 2008. doi: 10.1007/s10856-008-3498-y.
16. Anselme K, Linez P, Bigerelle M. The relative influence of the topography and chemistry of TiAl6V4 surfaces on osteoblastic cell behaviour. Biomaterials. 2000. doi: 10.1016/S0142-9612(00)00042-9.
17. van Kooten TG, Schakenraad JM. Influence of substratum wettability on the strength of adhesion of human fibroblasts. Biomaterials. 1992. doi: 10.1016/0142-9612(92)90112-2.
18. Kilpadi DV, Lemons JE. Surface-energy characterization of unalloyed titanium impants. J Biomed Mater Res. 1994. doi: 10.1002/jbm.820281206.
19. Ogorodnikov VV, Rogovoi YI. Rules of change in elastic, thermal, and energy properties in a number of cubic transition-metal monocrabides. Powder Metall Met Ceram. 1994. doi:10.1007/BF00561272.
20. Cornell WD, Cieplak P, Bayly CI. A second generation force field for the simulation of proteins, nucleic acids, and organic molecules. J Am Chem Soc. 1995. doi: 10.1021/ja00124a002.
21. Ryckaert JP, Ciccotti G, Berendsen HJC. Numerial integration of the cartesian equations of motion of a system with constriaints: molecular dynamics of n-alkanes. J Comp Phys. 1977. doi: 10.1016/0021-9991(77)90098-5.
22. Massaro C, Rotolo P, Riccardis FD, Milella E, Napoli A. Comparative investigation of the surface properties of commercial titanium dental implants. Part I: chemical composition. J Mater Sci: Mater Med. 2002;13:535–48.
23. Roddick-Lanzillotta AD, McQuillan AJ. An in situ infrared spectroscopic investigation of lysine peptide and polylysine adsorption to TiO_2 from aqueous solutions. J Colloid Interface Sci. 1999. doi: 10.1006/jcis.1999.6367.
24. Roddick-Lanzillotta AD, McQuillan AJ. An in situ infrared spectroscopic study of glutamic acid and of aspartic acid adsorbed on TiO_2: implications for the biocompatibility of titanium. J Colloid Interface Sci. 2000. doi: 10.1006/jcis.2000.6864.
25. Ponsonnet L, Comte V, Othmane A, Lagneau C, Charbonnier M, Lissac M, Jaffrezic N. Effect of surface topography and chemistry on adhesion, orientation and growth of fibroblasts on nickel-titanium substrates. Mater Sci Eng C. 2002. doi: 10.1016/S0928-4931(02)00097-8.
26. Clark P, Connolly P, Curtis ASG, Dow JAT, Wilkinson CDW. Topographical control of cell behavior: II. multiple grooved substrata. Development. 1990;108:635–44.